

---

# Neural Ensemble Search for Performant and Calibrated Predictions

---

Sheheryar Zaidi<sup>1\*</sup> Arber Zela<sup>2\*</sup> Thomas Elsken<sup>2</sup>  
Chris Holmes<sup>1</sup> Frank Hutter<sup>2,3</sup> Yee Whye Teh<sup>1</sup>

<sup>1</sup>University of Oxford, <sup>2</sup>University of Freiburg, <sup>3</sup>Bosch Center for Artificial Intelligence  
{szaidi, cholmes, y.w.teh}@stats.ox.ac.uk  
{zelaa, elsken, fh}@cs.uni-freiburg.de

## Abstract

Ensembles of neural networks achieve superior performance compared to stand-alone networks not only in terms of accuracy on in-distribution data but also on data with distributional shift alongside improved uncertainty calibration. Diversity among networks in an ensemble is believed to be key for building strong ensembles, but typical approaches only ensemble different weight vectors of a fixed architecture. Instead, we investigate neural architecture search (NAS) for explicitly constructing ensembles to exploit diversity among networks of varying architectures and to achieve robustness against distributional shift. By directly optimizing ensemble performance, our methods implicitly encourage diversity among networks, without the need to explicitly define diversity. We find that the resulting ensembles are more diverse compared to ensembles composed of a fixed architecture and are therefore also more powerful. We show significant improvements in ensemble performance on image classification tasks both for in-distribution data and during distributional shift with better uncertainty calibration.

## 1 Introduction

Automatically learning useful representations of data using deep neural networks has been successful across various tasks [30, 25, 40], leading to the ubiquitous deployment of neural networks. While some applications rely only on the predictions made by a neural network, many critical applications also require reliable predictive uncertainty estimates and robustness under the presence of distributional shift in the data observed at test time relative to the training data. Examples include medical imaging [16] and self-driving cars [6]. However, several studies have shown that neural networks are not always robust to dataset shift [43, 24], nor do they exhibit calibrated predictive uncertainty, resulting in overconfident and incorrect predictions [20].

Using an ensemble of networks rather than a stand-alone network is a strong baseline both in terms of predictive uncertainty calibration and robustness to dataset shift. Ensembles also outperform approximate Bayesian methods [33, 43, 21]. Their success is usually attributed to the diversity among the base learners, however there are various definitions of diversity [32, 63] without a consensus. In practice, ensembles are usually constructed by choosing a *fixed* state-of-the-art architecture, and creating base learners either by independently training random initializations of it (called *deep ensembles* [33]) or by picking various checkpoints of a single training trajectory [27, 37].

However, as we show, base learners with varying architectures make more diverse predictions. Therefore, picking a fixed architecture for the ensemble’s base learners neglects diversity in favor of base learner strength. This has implications for the ensemble performance, since both diversity and

---

\*Equal contribution.

base learner strength are important. To overcome this, we propose *Neural Ensemble Search* (NES); a NES algorithm finds a set of diverse neural architectures that together form a strong ensemble. By directly optimizing ensemble loss while maintaining independent training of base learners, a NES algorithm implicitly encourages diversity, without the need for explicitly defining the notion of diversity. In detail, our contributions are as follows:

1. We show that ensembles composed of varying architectures perform better than ensembles composed of a fixed architecture. We demonstrate that this is due to increased diversity among the ensemble’s base learners (Sections 3 and 5).
2. Based on these findings and the importance of diversity, we propose two algorithms for Neural Ensemble Search: NES-RS and NES-RE. NES-RS is a simple random search based algorithm, and NES-RE is based on regularized evolution [44]. Both search algorithms seek performant ensembles with varying base learner architectures (Section 4).
3. Through experiments on image classification tasks, we evaluate the ensembles found by NES-RS and NES-RE from the point of view of both predictive performance and uncertainty calibration. We also compare to the baseline of deep ensembles with fixed, optimized architectures. We find our ensembles outperform deep ensembles not only on in-distribution data but also during dataset shift, with better predictive performance and uncertainty calibration (Section 5).

The code for our experiments is available at: <https://github.com/automl/nas>.

## 2 Related Work

**Ensemble Learning.** Ensembles of neural networks [22, 31, 11] are commonly used to boost performance [50, 47, 23]. In practice, strategies for building ensembles include the popular approach of independently training multiple initializations of the same network, training base learners on bootstrap samples of the training data (i.e. *bagging*) [64], joint training with diversity-encouraging losses [34, 62, 52] and using checkpoints during the training trajectory of a network [27, 37]. We focus on ensembles of independently trained base learners, as this is a simple approach leading to strong ensembles (see [34] for a comparison of ensembling approaches). Diversity is believed to be key for successful ensembles and various proposals have been made for its definition [32], yet there is no consensus [63]. Much recent interest in ensembles has been due to their strong predictive uncertainty estimation [33], with extensive empirical studies observing that ensembles outperform other approaches for uncertainty estimation, notably including approximate Bayesian methods [43, 21].

**Neural Architecture Search.** Neural Architecture Search (NAS), the process of automatically designing neural network architectures, is a natural next step for automating the learning of representations with neural networks [15]. Existing strategies using reinforcement learning [2, 61, 65, 66], evolutionary algorithms [1, 14, 44, 45, 48] or Bayesian Optimization [29, 39, 42, 53] have demonstrated that NAS can find architectures that surpass hand-crafted ones on a variety of tasks. A recent focus in NAS research has been on computational efficiency with algorithms utilizing gradient-based optimization [8, 12, 36, 55, 59, 56], network morphisms [7, 13, 14], or multi-fidelity optimization [3, 17, 60].

A recent line of research which is closest to ours connects ensemble learning and NAS. Methods proposed by Cortes et al. [10] and Macko et al. [38] iteratively add (sub-)networks to an ensemble to improve the ensemble’s performance. While our work focuses on generating a diverse and well-performing (in an ensemble) set of architectures while essentially fixing the way an ensemble is built from its base learners, the focus of [10] and [38] is on how to build the ensemble. As a consequence, the space of neural networks they consider is limited in contrast to our work: [10] only considers fully-connected neural networks and [38] only uses NASNet-A [66] building blocks with varying depth and number of filters. Interestingly, [38] employs knowledge distillation [26], which is also used in NAS research [14, 46]. However, this can actively discourage diversity in predictions; therefore, we do not consider it in our work. Rather than iteratively growing an ensemble, Bian et al. [5] propose to prune redundant (sub-) networks in an ensemble without significant loss in performance by utilizing diversity. While all aforementioned work only focuses on performance for in-distribution data, we additionally consider dataset shift as well as uncertainty calibration.

### 3 Ensembles of Varying Architectures are More Diverse

After introducing our notation and problem set-up, we discuss diversity in ensembles of neural networks and provide empirical evidence that networks with varying architectures make more diverse predictions than networks with a fixed architecture trained multiple times.

#### 3.1 Definitions and Set-up

Let  $\mathcal{D}_{\text{train}} = \{(\mathbf{x}_i, y_i) : i = 1, \dots, N\}$  be the training dataset, where the input  $\mathbf{x}_i \in \mathbb{R}^D$  and, assuming a classification task, the output  $y_i \in \{1, \dots, C\}$ . We use  $\mathcal{D}_{\text{val}}$  and  $\mathcal{D}_{\text{test}}$  for the validation and test datasets, respectively. Denote by  $f_\theta$  a neural network with weights  $\theta$ , so  $f_\theta(\mathbf{x}) \in \mathbb{R}^C$  is the predicted probability vector over the classes for input  $\mathbf{x}$ . Let  $\ell(f_\theta(\mathbf{x}), y)$  be the neural network’s loss for data point  $(\mathbf{x}, y)$ . Given  $M$  networks  $f_{\theta_1}, \dots, f_{\theta_M}$ , we construct the *ensemble*  $F$  of these networks by averaging the outputs, yielding  $F(\mathbf{x}) = \frac{1}{M} \sum_{i=1}^M f_{\theta_i}(\mathbf{x})$ .

In addition to the ensemble’s loss  $\ell(F(\mathbf{x}), y)$ , we will also consider the *average base learner* loss and the *oracle ensemble’s* loss. The average base learner loss is simply defined as  $\frac{1}{M} \sum_{i=1}^M \ell(f_{\theta_i}(\mathbf{x}), y)$ ; we use this to measure the *average base learner strength*. Similar to [34, 62], the oracle ensemble  $F_{\text{OE}}$  composed of base learners  $f_{\theta_1}, \dots, f_{\theta_M}$  is defined to be the function which, given an input  $\mathbf{x}$ , returns the prediction of the base learner with the smallest loss for  $(\mathbf{x}, y)$ , that is,

$$F_{\text{OE}}(\mathbf{x}) = f_{\theta_k}(\mathbf{x}), \quad \text{where } k \in \underset{i}{\operatorname{argmin}} \ell(f_{\theta_i}(\mathbf{x}), y).$$

Of course, the oracle ensemble can only be constructed if the true class  $y$  is known. We use the oracle ensemble loss as a measure of the *diversity* in base learner predictions. Intuitively, if base learners make diverse predictions for  $\mathbf{x}$ , the oracle ensemble is more likely to find some base learner with a small loss, whereas if all base learners make identical predictions, the oracle ensemble yields the same output as any (and all) base learners. Therefore, as a rule of thumb, *small oracle ensemble loss indicates more diverse base learner predictions*.

**Proposition 3.1.** Suppose  $\ell$  is negative log-likelihood (NLL). Then, the oracle ensemble loss, ensemble loss, and average base learner loss satisfy the following inequality:

$$\ell(F_{\text{OE}}(\mathbf{x}), y) \leq \ell(F(\mathbf{x}), y) \leq \frac{1}{M} \sum_{i=1}^M \ell(f_{\theta_i}(\mathbf{x}), y).$$

We refer to Appendix A for a proof. Proposition 3.1 suggests that strong ensembles require not only strong average base learners (smaller upper bound), but also more diversity in their predictions (smaller lower bound). There is extensive theoretical work relating strong base learner performance and diversity with the generalization properties of ensembles [22, 63, 28, 4, 19]. Notably, Breiman [49] showed that the generalization error of random forests depends on the strength of individual trees and the correlation between their mistakes.

#### 3.2 Visualizing Similarity in Base Learner Predictions

In practice, ensembles of neural networks are usually made by independently training  $M$  random initializations of a network with a fixed architecture, on the same training dataset. This procedure is called *deep ensembles*, and has been empirically observed to yield performant and calibrated ensembles [33, 43].

The fixed architecture used to build deep ensembles is typically chosen to be a strong stand-alone architecture, either hand-crafted or found by NAS. However, since ensemble performance depends not only on strong base learners but also on their diversity, optimizing the base learner’s architecture and *then* constructing a deep ensemble neglects diversity in favor of strong base learner performance.

Having base learner architectures vary allows more diversity in their predictions. In this section, we provide empirical evidence for this by visualizing the base learners’ predictions. Fort et al. [18] found that base learners in a deep ensemble explore different parts of the function space by means of applying dimensionality reduction to their predictions. Building on this, we uniformly sample five architectures from the DARTS search space [36], train 20 initializations of each architecture on CIFAR-10 and visualize the similarity among the networks’ predictions on the test dataset using t-SNE [51]. Experiment details are available in Section 5 and Appendix B.

As shown in Figure 1a, we observe clustering of predictions made by different initializations of a fixed architecture, suggesting that base learners with varying architectures explore different parts of the function space. Moreover, we also visualize the predictions of base learners of two ensembles, each of size  $M = 30$ , where one is a deep ensemble (i.e. a fixed architecture trained multiple times) and the other has varying architectures (found by NES-RS which will be introduced in Section 4). Figure 1b shows more diversity in the ensemble with varying architectures than in the one with a fixed architecture.

## 4 Neural Ensemble Search

In this section, we propose the concept of *neural ensemble search* (NES). In summary, a NES algorithm optimizes the architectures of base learners in an ensemble to minimize ensemble loss.

Given a network  $f : \mathbb{R}^D \rightarrow \mathbb{R}^C$ , let  $\mathcal{L}(f, \mathcal{D}) = \sum_{(\mathbf{x}, y) \in \mathcal{D}} \ell(f(\mathbf{x}), y)$  be the loss of  $f$  over dataset  $\mathcal{D}$ . Given a set of base learners  $\{f_1, \dots, f_M\}$ , let `Ensemble` be the function which maps  $\{f_1, \dots, f_M\}$  to the ensemble  $F = \frac{1}{M} \sum_{i=1}^M f_i$  as defined in Section 3. To emphasize the architecture, we use the notation  $f_{\theta, \alpha}$  to denote a network with architecture  $\alpha \in \mathcal{A}$  and weights  $\theta$ , where  $\mathcal{A}$  is a space of architectures. A NES algorithm aims to solve the following optimization problem:

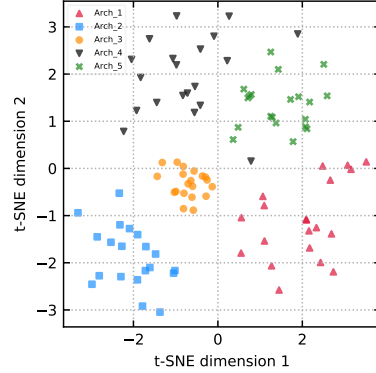
$$\begin{aligned} \min_{\alpha_1, \dots, \alpha_M \in \mathcal{A}} \mathcal{L}(\text{Ensemble}(f_{\theta_1, \alpha_1}, \dots, f_{\theta_M, \alpha_M}), \mathcal{D}_{\text{val}}) \quad (1) \\ \text{s.t. } \theta_i \in \operatorname{argmin}_{\theta} \mathcal{L}(f_{\theta, \alpha_i}, \mathcal{D}_{\text{train}}) \quad \text{for } i = 1, \dots, M \end{aligned}$$

Eq. 1 is difficult to solve for at least two reasons. First, we are optimizing over  $M$  architectures, so the search space is effectively  $\mathcal{A}^M$ , compared to it being  $\mathcal{A}$  in typical NAS, making it more difficult to explore fully. Second, a larger search space also increases the risk of overfitting the ensemble loss to  $\mathcal{D}_{\text{val}}$ . A possible approach here is to consider the ensemble as a single large network to which we apply NAS, but joint training of an ensemble through a single loss has been empirically observed to underperform training base learners independently, specially for large neural networks [52]. Instead, our general approach to solve Eq. 1 consists of two steps:

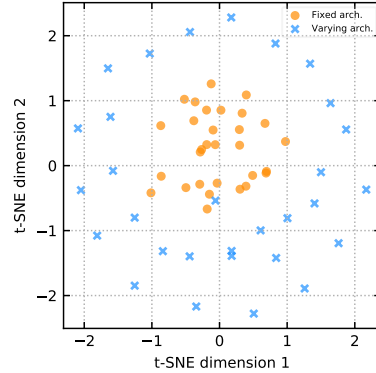
1. **Pool building:** build a *pool*  $\mathcal{P} = \{f_{\theta_1, \alpha_1}, \dots, f_{\theta_K, \alpha_K}\}$  of size  $K$  consisting of potential base learners, where each  $f_{\theta_i, \alpha_i}$  is a network trained independently on  $\mathcal{D}_{\text{train}}$ .
2. **Ensemble selection:** select  $M$  base learners  $f_{\theta_1^*, \alpha_1^*}, \dots, f_{\theta_M^*, \alpha_M^*}$  from  $\mathcal{P}$  to form an ensemble which minimizes loss on  $\mathcal{D}_{\text{val}}$ . (We assume  $K \geq M$ .)

Step 1 reduces the options for the base learner architectures, with the intention to make the search more feasible and focus on strong architectures. Step 2 then selects a performant ensemble which implicitly encourages base learner strength *and* diversity. This procedure also ensures that the ensemble’s base learners are trained independently. We propose using forward step-wise selection for step 2; that is, given the set of networks  $\mathcal{P}$ , we start with an empty ensemble and add to it the network from  $\mathcal{P}$  which minimizes ensemble loss on  $\mathcal{D}_{\text{val}}$ . We repeat this without replacement until the ensemble is of size  $M$ . Let `ForwardSelect`( $\mathcal{P}, \mathcal{D}_{\text{val}}, M$ ) denote the set of  $M$  base learners selected from  $\mathcal{P}$  by this procedure.

Note that selecting the ensemble from  $\mathcal{P}$  is a combinatorial optimization problem; a greedy approach such as `ForwardSelect` is nevertheless effective [9], while keeping computational overhead low, given the predictions of the networks on  $\mathcal{D}_{\text{val}}$ . We also experimented with three other ensemble selection algorithms: (1) Starting with the best network by validation performance, add the next best network to the ensemble only if it improves validation performance, iterating until the ensemble size



(a) Five different architectures, each trained with 20 different initializations.



(b) Predictions of base learners in two ensembles, one with fixed architecture and one with varying architectures.

Figure 1: t-SNE visualization of base learner predictions.

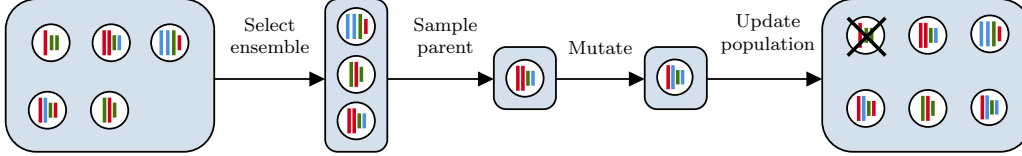


Figure 2: Illustration of one iteration of NES-RE. Network architectures are represented as colored bars of different lengths illustrating different layers and widths. Starting with the current population, ensemble selection is applied to select parent candidates, among which one is sampled as the parent. A mutated copy of the parent is added to the population, and the oldest member is removed.

is  $M$  or all models have been considered.<sup>2</sup> (2) Select the top  $M$  networks by validation performance. (3) Forward step-wise selection *with* replacement. We typically found that these three performed comparatively or worse than our choice `ForwardSelect`.

We have not yet discussed the algorithm for building the pool in step 1; we propose two approaches, NES-RS (Section 4.1) and NES-RE (Section 4.2). NES-RS is a simple random search based algorithm, while NES-RE is based on regularized evolution [44], a state-of-the-art NAS algorithm. Note that while gradient-based NAS methods have recently become popular, they are not naively applicable in our setting as the base learner selection component `ForwardSelect` is typically non-differentiable.

#### 4.1 NES with Random Search

In NAS, random search (RS) is a competitive baseline on carefully designed architecture search spaces [35, 57, 58]. Motivated by its success and simplicity, we first introduce NES with random search (NES-RS). NES-RS builds the pool  $\mathcal{P}$  by independently sampling architectures uniformly from the search space  $\mathcal{A}$  (and training them). Since the architectures of networks in  $\mathcal{P}$  vary, applying ensemble selection is a simple way to exploit diversity, yielding a performant ensemble. Algorithm 1 describes NES-RS in pseudocode.

---

#### Algorithm 1: NES with Random Search

---

**Data:** Search space  $\mathcal{A}$ ; ensemble size  $M$ ; comp. budget  $K$ ;  $\mathcal{D}_{\text{train}}$ ,  $\mathcal{D}_{\text{val}}$ .

- 1 Sample  $K$  architectures  $\alpha_1, \dots, \alpha_K$  independently and uniformly from  $\mathcal{A}$ .
  - 2 Train each architecture  $\alpha_i$  using  $\mathcal{D}_{\text{train}}$ , yielding a pool of networks  $\mathcal{P} = \{f_{\theta_1, \alpha_1}, \dots, f_{\theta_K, \alpha_K}\}$ .
  - 3 Select base learners  $\{f_{\theta_1^*, \alpha_1^*}, \dots, f_{\theta_M^*, \alpha_M^*}\} = \text{ForwardSelect}(\mathcal{P}, \mathcal{D}_{\text{val}}, M)$  by forward step-wise selection without replacement.
  - 4 **return** ensemble  $\text{Ensemble}(f_{\theta_1^*, \alpha_1^*}, \dots, f_{\theta_M^*, \alpha_M^*})$
- 

#### 4.2 NES with Regularized Evolution

A more guided approach for building the pool  $\mathcal{P}$  is using regularized evolution (RE) [44]. While RS has the benefit of simplicity, by sampling architectures uniformly, the resulting pool might contain many weak architectures, leaving few strong architectures for `ForwardSelect` to choose between. Therefore, NES-RS might require a large pool in order to explore interesting parts of the search space. RE is an evolutionary algorithm used for NAS which explores the search space by evolving a *population* of architectures. In summary, RE starts with a randomly initialized fixed-size population of architectures. At each iteration, a subset of size  $m$  of the population is sampled, from which the best network by validation loss is selected as the parent. A mutated copy of the parent architecture, called the child, is trained and added to the population, and the oldest member of the population is removed, preserving the population size. This is iterated until the computational budget is reached, returning the *history*, i.e. all the networks evaluated during the search.

Based on RE for NAS, we propose NES-RE to build the pool of potential base learners. NES-RE starts by randomly initializing a population  $\mathfrak{p}$  of size  $P$ . At each iteration, we apply `ForwardSelect` to the population to select an ensemble of size  $m$ , and we uniformly sample one base learner from the ensemble to be the parent. A mutated copy of the parent is added to  $\mathfrak{p}$  and the oldest network

<sup>2</sup>This approach returns an ensemble of size at most  $M$ .

---

**Algorithm 2:** NES with Regularized Evolution

---

**Data:** Search space  $\mathcal{A}$ ; ensemble size  $M$ ; comp. budget  $K$ ;  $\mathcal{D}_{\text{train}}, \mathcal{D}_{\text{val}}$ ; population size  $P$ ; number of parent candidates  $m$ .

- 1 Sample  $P$  architectures  $\alpha_1, \dots, \alpha_P$  independently and uniformly from  $\mathcal{A}$ .
- 2 Train each architecture  $\alpha_i$  using  $\mathcal{D}_{\text{train}}$ , and initialize  $\mathfrak{p} = \mathcal{P} = \{f_{\theta_1, \alpha_1}, \dots, f_{\theta_P, \alpha_P}\}$ .
- 3 **while**  $|\mathcal{P}| < K$  **do**
- 4     Select  $m$  parent candidates  $\{f_{\tilde{\theta}_1, \tilde{\alpha}_1}, \dots, f_{\tilde{\theta}_m, \tilde{\alpha}_m}\} = \text{ForwardSelect}(\mathfrak{p}, \mathcal{D}_{\text{val}}, m)$ .
- 5     Sample uniformly a parent architecture  $\alpha$  from  $\{\tilde{\alpha}_1, \dots, \tilde{\alpha}_m\}$ . // parent stays in  $\mathfrak{p}$ .
- 6     Apply mutation to  $\alpha$ , yielding child architecture  $\beta$ .
- 7     Train  $\beta$  using  $\mathcal{D}_{\text{train}}$  and add the trained network  $f_{\theta, \beta}$  to  $\mathfrak{p}$  and  $\mathcal{P}$ .
- 8     Remove the oldest member in  $\mathfrak{p}$ . // as done in RE [44].
- 9 Select base learners  $\{f_{\theta_1^*, \alpha_1^*}, \dots, f_{\theta_M^*, \alpha_M^*}\} = \text{ForwardSelect}(\mathcal{P}, \mathcal{D}_{\text{val}}, M)$  by forward step-wise selection without replacement.
- 10 **return** ensemble  $\text{Ensemble}(f_{\theta_1^*, \alpha_1^*}, \dots, f_{\theta_M^*, \alpha_M^*})$

---

is removed, as in regularized evolution. This process is repeated until the computational budget is reached, and the history is returned as the pool  $\mathcal{P}$ . See Algorithm 2 for pseudocode and Figure 2 for an illustration.

Also, note the distinction between the *population* and the *pool* in NES-RE: the population is evolved, whereas the pool is the set of all networks evaluated during evolution (i.e., the history) and is used post-hoc for selecting the ensemble. Moreover, `ForwardSelect` is used both for selecting  $m$  parent candidates (line 4 in NES-RE) and choosing the final ensemble of size  $M$  (line 9 in NES-RE). In general,  $m \neq M$ .

### 4.3 Ensemble Adaptation to Dataset Shift

Using deep ensembles is a common way of building a model robust to distributional shift relative to training data. In general, one may not know the type of distributional shift that occurs at test time. However, by using an ensemble, diversity in base learner predictions prevents the model from relying on one base learner’s predictions which may not only be incorrect but also overconfident.

We assume that one does not have access to data points with test-time shift at training time, but one does have access to some validation data  $\mathcal{D}_{\text{val}}^{\text{shift}}$  with a *validation* shift, which encapsulates one’s belief about test-time shift. A simple way to adapt NES-RS and NES-RE to return ensembles robust to shift is by using  $\mathcal{D}_{\text{val}}^{\text{shift}}$  instead of  $\mathcal{D}_{\text{val}}$  whenever applying `ForwardSelect` to select the final ensemble. In algorithms 1 and 2, this is in lines 3 and 9, respectively. Note that in line 4 of Algorithm 2, we can also replace  $\mathcal{D}_{\text{val}}$  with  $\mathcal{D}_{\text{val}}^{\text{shift}}$  when expecting test-time shift, however to avoid running NES-RE once for each of  $\mathcal{D}_{\text{val}}, \mathcal{D}_{\text{val}}^{\text{shift}}$ , we simply sample one of  $\mathcal{D}_{\text{val}}, \mathcal{D}_{\text{val}}^{\text{shift}}$  uniformly at each iteration, in order to explore architectures that work well both in-distribution and during shift. See Appendices C.2 and B.3 for further discussion.

## 5 Experiments

We apply NES using the cell-based search space for DARTS [36] and evaluate the ensembles found on two image classification datasets: Fashion-MNIST [54] and CIFAR-10-C [24]. CIFAR-10-C is a dataset based on CIFAR-10 but also includes validation and test dataset shifts, each with five severity levels. We use three metrics: NLL, classification error and expected calibration error (ECE) [20, 41]. Hyperparameter choices, experimental and implementation details are available in Appendix B. Note that we do not aim for state-of-the-art performance but rather focus on understanding the improvement over baselines based on deep ensembles. Unless stated otherwise, all evaluations are on the test dataset.

**Baselines.** We compare the ensembles found by NES to the baseline of deep ensembles built using a fixed, optimized architecture. The fixed architecture is either: (1) optimized by random search, called DeepEns (RS), (2) the architecture found using DARTS, called DeepEns (DARTS) or (3) the architecture found using RE, called DeepEns (AmoebaNet). All architectures used have five nodes

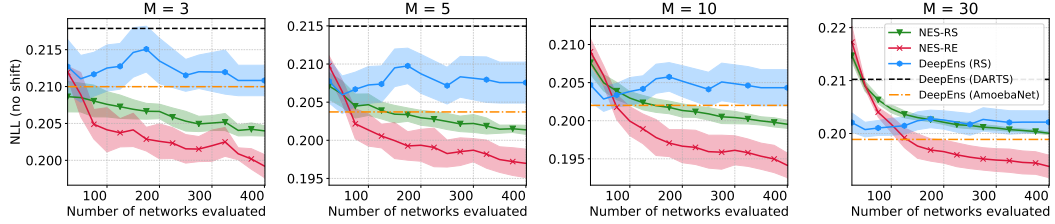


Figure 3: Results on Fashion-MNIST with varying ensemble sizes  $M$ . Lines show the mean NLL achieved by the ensembles with 95% confidence intervals.

in their cells, except AmoebaNet, which has six nodes. All base learners also use the same training routine. See Appendix B for details.

**Results on in-distribution data.** Figure 3 and the top row of Figure 4 show the NLL achieved by NES-RS, NES-RE and the baselines as a function of the computational budget  $K$  and ensemble size  $M$ . We see that NES algorithms consistently outperform the baselines, usually for most values of  $K$ . NES-RS and NES-RE perform comparably for CIFAR-10, but NES-RE outperforms NES-RS for Fashion-MNIST due to more efficient exploration of the search space. Interestingly, despite AmoebaNet being deeper, both NES algorithms outperform deep ensembles of AmoebaNet, except for NES-RS on Fashion-MNIST when  $M = 30$ , in which case the NLL is comparable.

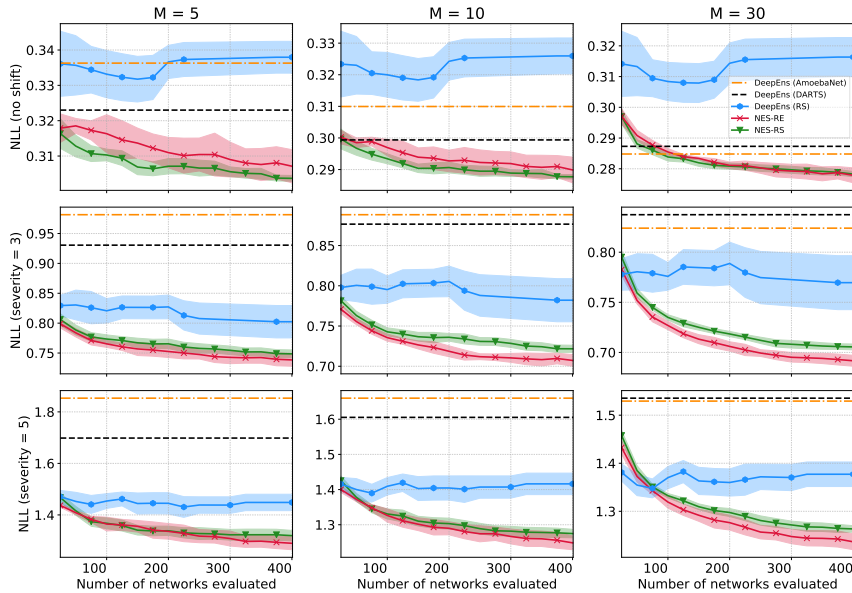


Figure 4: Results on CIFAR-10-C [24] with varying ensemble sizes  $M$  and shift severity. Lines show the mean NLL achieved by the ensembles with 95% confidence intervals.

**Results during dataset shift.** Next, we evaluate the robustness of the ensembles during dataset shift for CIFAR-10-C. All base learners are trained on  $\mathcal{D}_{\text{train}}$  without any form of data augmentation. However, we use a shifted validation dataset,  $\mathcal{D}_{\text{val}}^{\text{shift}}$ , and a shifted test dataset,  $\mathcal{D}_{\text{test}}^{\text{shift}}$ .  $\mathcal{D}_{\text{val}}^{\text{shift}}$  is built by applying a random *validation shift* to each datapoint in  $\mathcal{D}_{\text{val}}$ .  $\mathcal{D}_{\text{test}}^{\text{shift}}$  is built similarly but using instead *test shifts* applied to  $\mathcal{D}_{\text{test}}$  (see Appendix B and [24] for details). The severity of the shift varies between 1-5. The fixed architecture used in the baseline DeepEns (RS) is selected based on its loss over  $\mathcal{D}_{\text{val}}^{\text{shift}}$ , but the DARTS and AmoebaNet architectures remain unchanged.

As shown in the bottom two rows of Figure 4, ensembles picked by NES-RS and NES-RE are more robust to dataset shift than all three baselines. Unsurprisingly, DeepEns (DARTS) and DeepEns (AmoebaNet) perform poorly in comparison to the other methods, as they are not optimized to deal with dataset shift; the gap in performance naturally increases with shift severity, highlighting that highly optimized architectures can fail heavily under dataset shift. We also see that NES-RE improves over the performance of NES-RS during dataset shift.

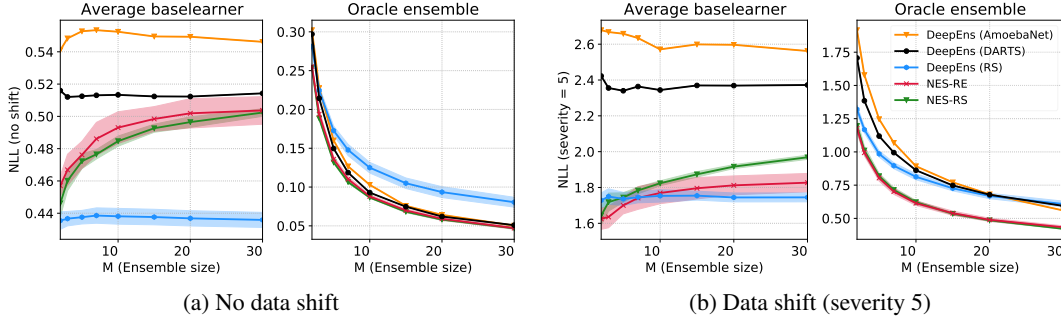


Figure 5: Results on CIFAR-10-C for the average base learner loss and the oracle ensemble loss (see Section 3 for details), with  $K = 400$ . Recall that small oracle ensemble loss generally corresponds to higher diversity.

**Classification error and uncertainty calibration.** We also assess the ensembles using classification error and expected calibration error (ECE). ECE measures whether the predicted probabilities are calibrated. Intuitively, whenever the ensemble makes a particular prediction with probability, e.g., 70%, one should expect the model to be correct around 70% of the times; ECE measures the extent of mismatch between the model’s confidence and accuracy. The results comparing NES-RE and NES-RS with baselines are shown in Table 1. In terms of classification error, we find that ensembles built by NES consistently outperform the baseline across ensemble sizes and shift severities, with reductions of up to 5 percentage points in error. As with loss, NES-RE outperforms NES-RS during dataset shift. We also see that ensembles found by NES exhibit superior uncertainty calibration, reducing ECE by up to 40% against baselines. Note that good uncertainty calibration is especially important when models are used during dataset shift.

Table 1: Error and ECE of ensembles on CIFAR-10-C for different shift severities and ensemble sizes  $M$  with  $K = 400$ . Best values and all values within 95% confidence interval are bold faced. See Table 3 for an extended version.

Shift Severity	$M$	Classification Error (out of 1)					Expected Calibration Error (ECE)				
		NES-RS	NES-RE	DeepEns (RS)	DeepEns (DARTS)	DeepEns (AmoebaNet)	NES-RS	NES-RE	DeepEns (RS)	DeepEns (DARTS)	DeepEns (AmoebaNet)
(no shift)	5	<b>0.098</b> $\pm$ 0.001	<b>0.098</b> $\pm$ 0.002	0.112 $\pm$ 0.002	0.101	<b>0.098</b>	<b>0.012</b> $\pm$ 0.001	<b>0.013</b> $\pm$ 0.002	<b>0.011</b> $\pm$ 0.002	0.015	0.016
	10	<b>0.094</b> $\pm$ 0.001	<b>0.094</b> $\pm$ 0.002	0.108 $\pm$ 0.002	0.100	0.097	<b>0.012</b> $\pm$ 0.001	0.013 $\pm$ 0.001	<b>0.011</b> $\pm$ 0.001	<b>0.011</b>	0.013
	30	<b>0.092</b> $\pm$ 0.001	<b>0.092</b> $\pm$ 0.001	0.105 $\pm$ 0.002	0.095	0.094	0.012 $\pm$ 0.001	0.012 $\pm$ 0.001	0.012 $\pm$ 0.001	<b>0.011</b>	0.012
3	5	0.238 $\pm$ 0.002	<b>0.233</b> $\pm$ 0.003	0.255 $\pm$ 0.007	0.266	0.267	<b>0.045</b> $\pm$ 0.002	<b>0.044</b> $\pm$ 0.002	0.062 $\pm$ 0.002	0.075	0.085
	10	0.232 $\pm$ 0.002	<b>0.229</b> $\pm$ 0.002	0.251 $\pm$ 0.007	0.263	0.256	<b>0.034</b> $\pm$ 0.001	<b>0.033</b> $\pm$ 0.002	0.052 $\pm$ 0.002	0.067	0.064
	30	0.231 $\pm$ 0.001	<b>0.228</b> $\pm$ 0.002	0.249 $\pm$ 0.007	0.258	0.252	<b>0.029</b> $\pm$ 0.001	<b>0.028</b> $\pm$ 0.002	0.049 $\pm$ 0.002	0.057	0.054
5	5	0.387 $\pm$ 0.003	<b>0.376</b> $\pm$ 0.003	0.415 $\pm$ 0.011	0.429	0.438	<b>0.117</b> $\pm$ 0.004	<b>0.115</b> $\pm$ 0.008	0.152 $\pm$ 0.002	0.177	0.199
	10	0.380 $\pm$ 0.002	<b>0.374</b> $\pm$ 0.004	0.411 $\pm$ 0.009	0.429	0.427	<b>0.104</b> $\pm$ 0.004	<b>0.105</b> $\pm$ 0.007	0.144 $\pm$ 0.002	0.168	0.174
	30	0.382 $\pm$ 0.002	<b>0.375</b> $\pm$ 0.003	0.408 $\pm$ 0.009	0.427	0.422	<b>0.103</b> $\pm$ 0.002	<b>0.102</b> $\pm$ 0.006	0.136 $\pm$ 0.003	0.160	0.160

**Diversity and average base learner strength.** To understand why ensembles found by NES algorithms outperform deep ensembles with fixed, optimized architectures, we view the ensembles through the lens of the average base learner loss and oracle ensemble loss as defined in Section 3, as shown in Figure 5. Recall that *small oracle ensemble loss indicates higher diversity*. We see that NES finds ensembles with smaller oracle ensemble losses indicating greater diversity among base learners. Unsurprisingly, the average base learner is weaker for NES as compared to DeepEns (RS). Despite this, the ensemble performs better, highlighting once again the importance of diversity.

## 6 Conclusion

We showed that ensembles with varying architectures are more diverse than ensembles with fixed architectures and argued that deep ensembles with fixed, optimized architectures neglect diversity. To this end, we proposed *Neural Ensemble Search*, which exploits diversity between base learners of varying architectures to find strong ensembles. We demonstrated empirically that NES-RE and NES-RS outperform deep ensembles in terms of both predictive performance and uncertainty calibration, for in-distribution data and also during dataset shift. We found that even NES-RS, a simple random search based algorithm, found ensembles capable of outperforming deep ensembles built with state-of-the-art architectures.

## Acknowledgments

AZ, TE and FH acknowledge support by the European Research Council (ERC) under the European Union Horizon 2020 research and innovation programme through grant no. 716721, and by BMBF grant DeToL. SZ acknowledges support from Aker Scholarship. CH wishes to acknowledge support from The Alan Turing Institute, The Medical Research Council UK, and the EPSRC Bayes4Health grant. We also thank Julien Siems for providing a parallel implementation of regularized evolution.

## References

- [1] Noor Awad, Neeratyoy Mallik, and Frank Hutter. Differential Evolution for Neural Architecture Search. *ICLR Neural Architecture Search Workshop*, 2020.
- [2] Bowen Baker, Otkrist Gupta, Nikhil Naik, and Ramesh Raskar. Designing Neural Network Architectures using Reinforcement Learning. *ICLR*, 2017.
- [3] Bowen Baker, Otkrist Gupta, Ramesh Raskar, and Nikhil Naik. Accelerating Neural Architecture Search using Performance Prediction. In *NIPS Workshop on Meta-Learning*, 2017.
- [4] Yijun Bian and Huanhuan Chen. When does Diversity Help Generalization in Classification Ensembles? *ArXiv*, abs/1903.06236, 2019.
- [5] Yijun Bian, Qingquan Song, Mengnan Du, Jun Yao, Huanhuan Chen, and Xia Hu. Sub-Architecture Ensemble Pruning in Neural Architecture Search. *ArXiv*, abs/1910.00370, 2019.
- [6] Mariusz Bojarski, Davide Del Testa, Daniel Dworakowski, Bernhard Firner, Beat Flepp, Prasoon Goyal, Lawrence D. Jackel, Mathew Monfort, Urs Muller, Jiakai Zhang, Xin Zhang, Jake Zhao, and Karol Zieba. End to End Learning for Self-Driving Cars. *CoRR*, abs/1604.07316, 2016.
- [7] Han Cai, Tianyao Chen, Weinan Zhang, Yong Yu, and Jun Wang. Efficient Architecture Search by Network Transformation. In *Association for the Advancement of Artificial Intelligence*, 2018.
- [8] Han Cai, Ligeng Zhu, and Song Han. ProxylessNAS: Direct Neural Architecture Search on Target Task and Hardware. In *International Conference on Learning Representations*, 2019.
- [9] Rich Caruana, Alexandru Niculescu-Mizil, Geoff Crew, and Alex Ksikes. Ensemble Selection from Libraries of Models. In *Proceedings of the Twenty-First International Conference on Machine Learning*, ICML '04, page 18, New York, NY, USA, 2004. Association for Computing Machinery.
- [10] Corinna Cortes, Xavier Gonzalvo, Vitaly Kuznetsov, Mehryar Mohri, and Scott Yang. AdaNet: Adaptive Structural Learning of Artificial Neural Networks. In *Proceedings of the 34th International Conference on Machine Learning*, volume 70 of *Proceedings of Machine Learning Research*, pages 874–883, International Convention Centre, Sydney, Australia, 06–11 Aug 2017. PMLR.
- [11] Thomas G. Dietterich. Ensemble Methods in Machine Learning. In *Multiple Classifier Systems*, pages 1–15, Berlin, Heidelberg, 2000. Springer Berlin Heidelberg.
- [12] Xuanyi Dong and Yi Yang. Searching for a Robust Neural Architecture in Four GPU Hours. In *Computer Vision and Pattern Recognition (CVPR)*, pages 1761–1770, 2019.
- [13] Thomas Elsken, Jan Hendrik Metzen, and Frank Hutter. Simple and Efficient Architecture Search for Convolutional Neural Networks. In *NeurIPS Workshop on Meta-Learning*, 2017.
- [14] Thomas Elsken, Jan Hendrik Metzen, and Frank Hutter. Efficient Multi-Objective Neural Architecture Search via Lamarckian Evolution. In *International Conference on Learning Representations*, 2019.
- [15] Thomas Elsken, Jan Hendrik Metzen, and Frank Hutter. Neural Architecture Search: A Survey. *Journal of Machine Learning Research*, 20(55):1–21, 2019.
- [16] Andre Esteva, Brett Kuprel, Roberto A. Novoa, Justin Ko, Susan M. Swetter, Helen M. Blau, and Sebastian Thrun. Dermatologist-level classification of skin cancer with deep neural networks. *Nature*, 542:115–, 2017.
- [17] Stefan Falkner, Aaron Klein, and Frank Hutter. BOHB: Robust and Efficient Hyperparameter Optimization at Scale. In *Proceedings of the 35th International Conference on Machine Learning*, volume 80 of *Proceedings of Machine Learning Research*, pages 1437–1446, Stockholmsmässan, Stockholm Sweden, 10–15 Jul 2018. PMLR.

- [18] Stanislav Fort, Huiyi Hu, and Balaji Lakshminarayanan. Deep Ensembles: A Loss Landscape Perspective. *ArXiv*, abs/1912.02757, 2019.
- [19] Ian Goodfellow, Yoshua Bengio, and Aaron Courville. *Deep Learning*. MIT Press, 2016.
- [20] Chuan Guo, Geoff Pleiss, Yu Sun, and Kilian Q. Weinberger. On Calibration of Modern Neural Networks. In *Proceedings of the 34th International Conference on Machine Learning*, volume 70 of *Proceedings of Machine Learning Research*, pages 1321–1330, International Convention Centre, Sydney, Australia, 06–11 Aug 2017. PMLR.
- [21] Fredrik K Gustafsson, Martin Danelljan, and Thomas B Schön. Evaluating Scalable Bayesian Deep Learning Methods for Robust Computer Vision. In *The IEEE Conference on Computer Vision and Pattern Recognition (CVPR) Workshops*, June 2020.
- [22] Lars K. Hansen and Peter Salamon. Neural network ensembles. *IEEE Transactions on Pattern Analysis and Machine Intelligence*, 12(10):993–1001, 1990.
- [23] Kaiming He, Xiangyu Zhang, Shaoqing Ren, and Jian Sun. Deep Residual Learning for Image Recognition. In *Proceedings of the IEEE Conference on Computer Vision and Pattern Recognition*, pages 770–778, 2016.
- [24] Dan Hendrycks and Thomas Dietterich. Benchmarking Neural Network Robustness to Common Corruptions and Perturbations. In *International Conference on Learning Representations*, 2019.
- [25] G. Hinton, L. Deng, D. Yu, G. E. Dahl, A. Mohamed, N. Jaitly, A. Senior, V. Vanhoucke, P. Nguyen, T. N. Sainath, and B. Kingsbury. Deep neural networks for acoustic modeling in speech recognition: The shared views of four research groups. *IEEE Signal Processing Magazine*, 29(6):82–97, 2012.
- [26] Geoffrey Hinton, Oriol Vinyals, and Jeff Dean. Distilling the Knowledge in a Neural Network. *ArXiv preprint*, abs/1503.02531, 2015.
- [27] Gao Huang, Yixuan Li, Geoff Pleiss, Zhuang Liu, John Hopcroft, and Kilian Weinberger. Snapshot Ensembles: Train 1, get m for free. In *International Conference on Learning Representations*, 2017.
- [28] Zhengshen Jiang, Hongzhi Liu, Bin Fu, and Zhonghai Wu. Generalized Ambiguity Decompositions for Classification with Applications in Active Learning and Unsupervised Ensemble Pruning. In *AAAI*, pages 2073–2079. AAAI Press, 2017.
- [29] Kirthevasan Kandasamy, Willie Neiswanger, Jeff Schneider, Barnabas Poczos, and Eric P Xing. Neural Architecture Search with Bayesian Optimisation and Optimal Transport. In *Advances in Neural Information Processing Systems*, pages 2016–2025, 2018.
- [30] Alex Krizhevsky, Ilya Sutskever, and Geoffrey E Hinton. Imagenet Classification with Deep Convolutional Neural Networks. In F. Pereira, C. J. C. Burges, L. Bottou, and K. Q. Weinberger, editors, *Advances in Neural Information Processing Systems 25*, pages 1097–1105. Curran Associates, Inc., 2012.
- [31] Anders Krogh and Jesper Vedelsby. Neural Network Ensembles, Cross Validation, and Active Learning. In G. Tesauero, D. S. Touretzky, and T. K. Leen, editors, *Advances in Neural Information Processing Systems 7*, pages 231–238. MIT Press, 1995.
- [32] Ludmila Kuncheva and Chris Whitaker. Measures of Diversity in Classifier Ensembles and Their Relationship with the Ensemble Accuracy. *Machine Learning*, 51:181–207, 05 2003.
- [33] Balaji Lakshminarayanan, Alexander Pritzel, and Charles Blundell. Simple and Scalable Predictive Uncertainty Estimation using Deep Ensembles. In *Advances in Neural Information Processing Systems 30*, pages 6402–6413. Curran Associates, Inc., 2017.
- [34] Stefan Lee, Senthil Purushwalkam, Michael Cogswell, David Crandall, and Dhruv Batra. Why M Heads are Better than One: Training a Diverse Ensemble of Deep Networks. *arXiv e-prints*, page arXiv:1511.06314, 2015.
- [35] Liam Li and Ameet Talwalkar. Random Search and Reproducibility for Neural Architecture Search. In *UAI*, page 129. AUAI Press, 2019.
- [36] Hanxiao Liu, Karen Simonyan, and Yiming Yang. DARTS: Differentiable Architecture Search. In *International Conference on Learning Representations*, 2019.
- [37] Ilya Loshchilov and Frank Hutter. SGDR: Stochastic Gradient Descent with Warm Restarts. In *International Conference on Learning Representations*, 2017.

- [38] Vladimir Macko, Charles Weill, Hanna Mazzawi, and Javier Gonzalvo. Improving Neural Architecture Search Image Classifiers via Ensemble Learning. *ArXiv*, abs/1903.06236, 2019.
- [39] Hector Mendoza, Aaron Klein, Matthias Feurer, Jost Tobias Springenberg, and Frank Hutter. Towards Automatically-Tuned Neural Networks. In *ICML 2016 AutoML Workshop*, 2016.
- [40] Tomas Mikolov, Ilya Sutskever, Kai Chen, Greg S Corrado, and Jeff Dean. Distributed Representations of Words and Phrases and their Compositionality. In *Advances in Neural Information Processing Systems 26*, pages 3111–3119. Curran Associates, Inc., 2013.
- [41] Mahdi Pakdaman Naeni, Gregory F. Cooper, and Milos Hauskrecht. Obtaining Well Calibrated Probabilities using Bayesian Binning. In *Proceedings of the Twenty-Ninth AAAI Conference on Artificial Intelligence*, AAAI’15, page 2901–2907. AAAI Press, 2015.
- [42] Changyong Oh, Jakub Tomczak, Efstratios Gavves, and Max Welling. Combinatorial Bayesian Optimization using the Graph Cartesian Product. In *Advances in Neural Information Processing Systems 32*, pages 2914–2924. Curran Associates, Inc., 2019.
- [43] Yaniv Ovadia, Emily Fertig, Jie Ren, Zachary Nado, D. Sculley, Sebastian Nowozin, Joshua Dillon, Balaji Lakshminarayanan, and Jasper Snoek. Can you trust your model’s uncertainty? Evaluating predictive uncertainty under dataset shift. In *Advances in Neural Information Processing Systems 32*, pages 13991–14002. Curran Associates, Inc., 2019.
- [44] Esteban Real, Alok Aggarwal, Yanping Huang, and Quoc V. Le. Regularized Evolution for Image Classifier Architecture Search. In *AAAI*, pages 4780–4789. AAAI Press, 2019.
- [45] Esteban Real, Sherry Moore, Andrew Selle, Saurabh Saxena, Yutaka Leon Suematsu, Jie Tan, Quoc V. Le, and Alexey Kurakin. Large-Scale Evolution of Image Classifiers. In *Proceedings of the 34th International Conference on Machine Learning*, volume 70 of *Proceedings of Machine Learning Research*, pages 2902–2911, International Convention Centre, Sydney, Australia, 06–11 Aug 2017. PMLR.
- [46] Christoph Schorn, Thomas Elsken, Sebastian Vogel, Armin Runge, Andre Gunto, and Gerd Ascheid. Automated design of error-resilient and hardware-efficient deep neural networks. *ArXiv preprint arXiv:1909.13844*, 2019.
- [47] Karen Simonyan and Andrew Zisserman. Very Deep Convolutional Networks for Large-Scale Image Recognition. In *International Conference on Learning Representations*, 2015.
- [48] Kenneth O Stanley and Risto Miikkulainen. Evolving neural networks through augmenting topologies. *Evolutionary Computation*, 10:99–127, 2002.
- [49] Leo Breiman Statistics and Leo Breiman. Random forests. In *Machine Learning*, pages 5–32, 2001.
- [50] Christian Szegedy, Wei Liu, Yangqing Jia, Pierre Sermanet, Scott Reed, Dragomir Anguelov, Dumitru Erhan, Vincent Vanhoucke, and Andrew Rabinovich. Going Deeper with Convolutions. In *Computer Vision and Pattern Recognition (CVPR)*, 2015.
- [51] Laurens Van der Maaten and Geoffrey Hinton. Visualizing data using t-SNE. *Journal of Machine Learning Research*, 9(2579-2605):85, 2008.
- [52] Andrew M. Webb, Charles Reynolds, Dan-Andrei Iliescu, Henry W. J. Reeve, Mikel Luján, and Gavin Brown. Joint Training of Neural Network Ensembles. *CoRR*, abs/1902.04422, 2019.
- [53] Colin White, Willie Neiswanger, and Yash Savani. BANANAS: Bayesian Optimization with Neural Networks for Neural Architecture Search, 2020.
- [54] Han Xiao, Kashif Rasul, and Roland Vollgraf. Fashion-MNIST: A Novel Image Dataset for Benchmarking Machine Learning Algorithms. *arXiv e-prints*, 2017.
- [55] Sirui Xie, Hehui Zheng, Chunxiao Liu, and Liang Lin. SNAS: Stochastic Neural Architecture Search. In *International Conference on Learning Representations*, 2019.
- [56] Yuhui Xu, Lingxi Xie, Xiaopeng Zhang, Xin Chen, Guo-Jun Qi, Qi Tian, and Hongkai Xiong. PC-DARTS: Partial Channel Connections for Memory-Efficient Architecture Search. In *International Conference on Learning Representations*, 2020.
- [57] Antoine Yang, Pedro M. Esperança, and Fabio M. Carlucci. NAS evaluation is frustratingly hard. In *International Conference on Learning Representations*, 2020.

- [58] Kaicheng Yu, Christian Sciuto, Martin Jaggi, Claudiu Musat, and Mathieu Salzmann. Evaluating the Search Phase of Neural Architecture Search. In *International Conference on Learning Representations*, 2020.
- [59] Arber Zela, Thomas Elsken, Tonmoy Saikia, Yassine Marrakchi, Thomas Brox, and Frank Hutter. Understanding and Robustifying Differentiable Architecture Search. In *International Conference on Learning Representations*, 2020.
- [60] Arber Zela, Aaron Klein, Stefan Falkner, and Frank Hutter. Towards Automated Deep Learning: Efficient Joint Neural Architecture and Hyperparameter Search. In *ICML Workshop on AutoML*, 2018.
- [61] Zhao Zhong, Junjie Yan, Wei Wu, Jing Shao, and Cheng-Lin Liu. Practical Block-wise Neural Network Architecture Generation. In *Proceedings of the IEEE Conference on Computer Vision and Pattern Recognition*, pages 2423–2432, 2018.
- [62] Tianyi Zhou, Shengjie Wang, and Jeff A Bilmes. Diverse Ensemble Evolution: Curriculum Data-Model Marriage. In *Advances in Neural Information Processing Systems 31*, pages 5905–5916. Curran Associates, Inc., 2018.
- [63] Zhi-Hua Zhou. *Ensemble Methods: Foundations and Algorithms*. Chapman & Hall, 1st edition, 2012.
- [64] Zhi-Hua Zhou, Jianxin Wu, and Wei Tang. Ensembling neural networks: Many could be better than all. *Artificial Intelligence*, 137(1):239 – 263, 2002.
- [65] Barret Zoph and Quoc V Le. Neural Architecture Search with Reinforcement Learning. In *International Conference on Learning Representations*, 2017.
- [66] Barret Zoph, Vijay Vasudevan, Jonathon Shlens, and Quoc V Le. Learning Transferable Architectures for Scalable Image Recognition. In *Proceedings of the IEEE Conference on Computer Vision and Pattern Recognition*, pages 8697–8710, 2018.

## A Proof of Proposition 3.1

Taking the loss function to be NLL, we have  $\ell(f(\mathbf{x}), y) = -\log [f(\mathbf{x})]_y$ , where  $[f(\mathbf{x})]_y$  is the probability assigned by the network  $f$  of  $\mathbf{x}$  belonging to the true class  $y$ , i.e. indexing the predicted probabilities  $f(\mathbf{x})$  with the true target  $y$ . Note that  $t \mapsto -\log t$  is a convex and decreasing function.

We first prove  $\ell(F_{\text{OE}}(\mathbf{x}), y) \leq \ell(F(\mathbf{x}), y)$ . Recall, by definition of  $F_{\text{OE}}$ , we have  $F_{\text{OE}}(\mathbf{x}) = f_{\theta_k}(\mathbf{x})$  where  $k \in \operatorname{argmin}_i \ell(f_{\theta_i}(\mathbf{x}), y)$ , therefore  $[F_{\text{OE}}(\mathbf{x})]_y = [f_{\theta_k}(\mathbf{x})]_y \geq [f_{\theta_i}(\mathbf{x})]_y$  for all  $i = 1, \dots, C$ . That is,  $f_{\theta_k}$  assigns the highest probability to the correct class  $y$  for input  $\mathbf{x}$ . Since  $-\log$  is a decreasing function, we have

$$\ell(F(\mathbf{x}), y) = -\log \left( \frac{1}{M} \sum_{i=1}^M [f_{\theta_i}(\mathbf{x})]_y \right) \geq -\log ([f_{\theta_k}(\mathbf{x})]_y) = \ell(F_{\text{OE}}(\mathbf{x}), y).$$

We apply Jensen’s inequality in its finite form for the second inequality. Jensen’s inequality states that for a real-valued, convex function  $\varphi$  with its domain being a subset of  $\mathbb{R}$  and numbers  $t_1, \dots, t_n$  in its domain,  $\varphi(\frac{1}{n} \sum_{i=1}^n t_i) \leq \frac{1}{n} \sum_{i=1}^n \varphi(t_i)$ . Noting that  $-\log$  is a convex function,  $\ell(F(\mathbf{x}), y) \leq \frac{1}{M} \sum_{i=1}^M \ell(f_{\theta_i}(\mathbf{x}), y)$  follows directly.

## B Experimental and Implementation Details

We describe details of the experiments shown in Section 5 and Appendix C. Note that unless stated otherwise, all sampling over a discrete set is done uniformly in the discussion below.

### B.1 Architecture Search Space

We use the same architecture search space as in DARTS [36]; denote this by  $\mathcal{A}$ . In  $\mathcal{A}$ , we search for two types of *cells*: *normal* cells, which preserve the spatial dimensions, and *reduction* cells, which reduce the spatial dimensions. These cells are stacked using a pre-determined macro-architecture where they are usually repeated and connected using additional skip connections. Each cell is a directed acyclic graph, where nodes represent feature maps in the computational graph and edges between them correspond to operation choices (e.g. a convolution operation). The cell parses inputs from the previous and previous-previous cells in its 2 input nodes. Afterwards it contains 5 nodes: 4 intermediate nodes that aggregate the information coming from 2 previous nodes in the cell and finally an output node that concatenates the output of all intermediate nodes across the channel dimension. AmoebaNet contains one more intermediate node, making that a deeper architecture. The set of possible operations (eight in total in DARTS) that we use for each edge in the cells is the same as DARTS, but we leave out the “zero” operation since that is not necessary for non-differentiable approaches such as random search and evolution. We refer the reader to [36] for more details.

### B.2 Training Routine

The macro-architecture we use has 16 initial channels and 8 cells (6 normal and 2 reduction), and was trained using a batch size of 100 for 100 epochs for CIFAR-10-C and 15 epochs for Fashion-MNIST. Unlike DARTS, we do not use any data augmentation procedure during training, nor any additional regularization such as ScheduledDropPath [66] or auxiliary heads. All other hyperparameter settings are exactly as in DARTS [36].

We split the training data of Fashion-MNIST with 50k samples being used for training base learners and 10k samples reserved for validation, which is used by the NES algorithms during ensemble selection and by DeepEns (RS) for picking the best architecture to use in the deep ensemble. We also set aside a test set with 10k samples; note that this test set is of course never used apart from evaluating the final ensembles. Similarly, we split CIFAR-10-C into 40k, 10k and 10k samples used for training, validation and testing, respectively. Note that when considering dataset shift for CIFAR-10-C, we also apply two disjoint sets of “corruptions” (following the terminology used by [24]) to the validation and test sets. We never apply any corruption to the training data. More specifically, out of the 19 different corruptions provided by [24], we randomly apply one from {Speckle Noise, Gaussian Blur, Spatter, Saturate} to each data point in the validation set and one from {Gaussian Noise, Shot Noise, Impulse Noise, Defocus Blur, Glass Blur,

Motion Blur, Zoom Blur, Snow, Frost, Fog, Brightness, Contrast, Elastic Transform, Pixelate, JPEG compression} to each data point in the test set. This choice of validation and test corruptions follows the recommendation of [24]. Also, as mentioned in Section 5, each of these corruptions have 5 severity levels, which yields 5 corresponding severity levels for  $\mathcal{D}_{\text{val}}^{\text{shift}}$  and  $\mathcal{D}_{\text{test}}^{\text{shift}}$ .

For NES-RE, NES-RS and DeepEns (RS), the results shown are averaged over multiple runs of each algorithm, with error bars showing the 95% confidence interval. For NES-RS and DeepEns (RS) on CIFAR-10-C and Fashion-MNIST, we sampled 1,200 random architectures first, then we sampled 400 architectures without replacement from these 1,200 for each run (because we used a maximum budget of 400 architecture evaluations) with a total of 10 runs. This was done in order to avoid training a very large number of networks. For NES-RE on CIFAR-10-C, we used a total of 6 independent runs, and for NES-RE on Fashion-MNIST, we used a total of 5 independent runs. Also, whenever the results do not have the computational budget on one of the axes (e.g. Figure 5), the budget for NES-RS, NES-RE and DeepEns (RS) is 400 architecture evaluations.

### B.3 Implementation Details of NES-RE

**Parallization.** Running NES-RE on a single GPU requires evaluating hundreds of networks sequentially, which is tedious. To circumvent this, we distribute the “while  $|\mathcal{P}| < K$ ” loop in Algorithm 2 over multiple GPUs, called worker nodes. We use the parallelism scheme provided by the `hpbandsster` [17] codebase.<sup>3</sup> In brief, the master node keeps track of the population and history (lines 1, 4-6, 8 in Algorithm 2), and it distributes the training of the networks to the individual worker nodes (lines 2, 7 in Algorithm 2). In our experiments, we always use 20 worker nodes and evolve a population  $\mathfrak{p}$  of size  $P = 50$ . During iterations of evolution, we use an ensemble size of  $m = 10$  to select parent candidates.

**Mutations.** We adapt the mutations used in RE to the DARTS search space. As in RE, we first pick a normal or reduction cell at random to mutate and then sample one of the following mutations:

- `identity`: no mutation is applied to the cell.
- `op mutation`: sample one edge in the cell and replace its operation with another operation sampled from the list of operations.
- `hidden state mutation`: sample one intermediate node in the cell, then sample one of its two incoming edges. Replace the input node of that edge with another sampled node, without altering the edge’s operation.

See [44] for details and illustrations of these mutations.

**Adaptation of NES-RE to dataset shifts.** As described in Section 4.3, at each iteration of evolution, the validation set used in line 4 of Algorithm 2 is sampled uniformly between  $\mathcal{D}_{\text{val}}$  and  $\mathcal{D}_{\text{val}}^{\text{shift}}$  when dealing with dataset shift. In this case, we use shift severity level 5 for  $\mathcal{D}_{\text{val}}^{\text{shift}}$ . Once the evolution is complete and the pool  $\mathcal{P}$  has been formed, then for each severity level  $s \in \{0, 1, \dots, 5\}$ , we apply `ForwardSelect` with  $\mathcal{D}_{\text{val}}^{\text{shift}}$  of severity  $s$  to select an ensemble from  $\mathcal{P}$  (line 9 in Algorithm 2), which is then evaluated on  $\mathcal{D}_{\text{test}}^{\text{shift}}$  of severity  $s$ . (Here  $s = 0$  corresponds to no shift.) This only applies to CIFAR-10-C, as we do not consider dataset shift for Fashion-MNIST.

## C Additional Experiments

In this section we provide additional results for the experiments conducted in Section 5. Note that, as with all results shown in Section 5, all evaluations are made on test data unless stated otherwise.

### C.1 Additional Results on Fashion-MNIST

To understand why NES algorithms outperform deep ensembles on Fashion-MNIST [54], we compare the average base learner loss (Figure 6) and oracle ensemble loss (Figure 7) of NES-RS, NES-RE and DeepEns (RS). Notice that, apart from the case when ensemble size  $M = 30$ , NES-RS and NES-RE

<sup>3</sup><https://github.com/automl/HpBandSter>

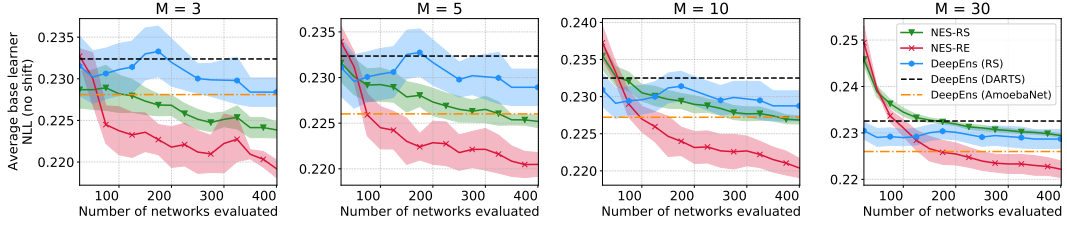


Figure 6: Average base learner loss for NES-RS, NES-RE and DeepEns (RS) on Fashion-MNIST. Lines show the mean NLL and 95% confidence intervals.

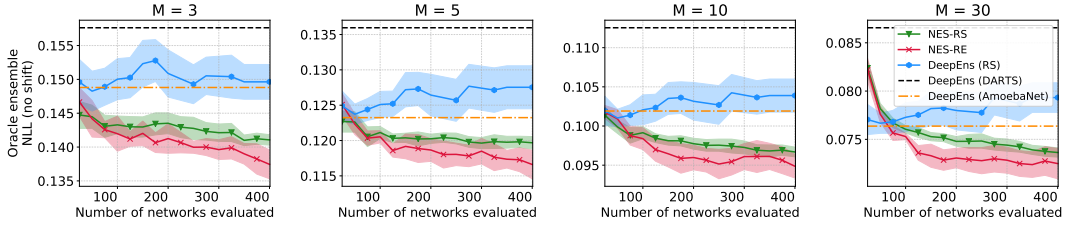


Figure 7: Oracle ensemble loss for NES-RS, NES-RE and DeepEns (RS) on Fashion-MNIST. Lines show the mean NLL and 95% confidence intervals.

find ensembles with both stronger and more diverse base learners (smaller losses in Figures 6 and 7, respectively). While it is expected that the oracle ensemble loss is smaller for NES-RS and NES-RE compared to DeepEns (RS), it initially appears surprising that DeepEns (RS) has a larger average base learner loss considering that the architecture for the deep ensemble is chosen to minimize the base learner loss. We found that this is due to the loss having a sensitive dependence not only on the architecture but also the initialization of the base learner networks. Therefore, re-training the best architecture by validation loss to build the deep ensemble yields base learners with higher losses due to the use of different random initializations. Fortunately, NES algorithms are not affected by this, since they simply select the ensemble’s base learners from the pool without having to re-train anything which allows them to exploit good architectures as well as initializations. Note that, for CIFAR-10-C experiments, this was not the case; base learner losses did not have as sensitive a dependence on the initialization as they did on the architecture.

In Table 2, we compare the classification error and expected calibration error (ECE) of NES algorithms with the deep ensembles baseline for various ensemble sizes on Fashion-MNIST. Similar to the loss, NES algorithms also achieve smaller errors, while ECE remains approximately the same for all methods.

Table 2: Error and ECE of ensembles on Fashion-MNIST for different ensemble sizes  $M$ . Best values and all values within 95% confidence interval are bold faced.

$M$	Classification Error (out of 1)					Expected Calibration Error (ECE)				
	NES-RS	NES-RE	DeepEns (RS)	DeepEns (DARTS)	DeepEns (AmoebaNet)	NES-RS	NES-RE	DeepEns (RS)	DeepEns (DARTS)	DeepEns (AmoebaNet)
3	0.074 $\pm$ 0.001	<b>0.072</b> $\pm$ 0.001	0.076 $\pm$ 0.001	0.077	0.077	0.007 $\pm$ 0.001	0.007 $\pm$ 0.002	0.008 $\pm$ 0.001	<b>0.003</b>	0.008
5	<b>0.073</b> $\pm$ 0.001	<b>0.071</b> $\pm$ 0.002	0.075 $\pm$ 0.001	0.077	0.074	<b>0.005</b> $\pm$ 0.001	<b>0.005</b> $\pm$ 0.001	<b>0.006</b> $\pm$ 0.001	<b>0.005</b>	<b>0.005</b>
10	0.073 $\pm$ 0.001	<b>0.070</b> $\pm$ 0.001	0.075 $\pm$ 0.001	0.076	0.073	<b>0.004</b> $\pm$ 0.001	<b>0.005</b> $\pm$ 0.001	<b>0.005</b> $\pm$ 0.001	0.006	<b>0.005</b>
30	0.073 $\pm$ 0.001	<b>0.070</b> $\pm$ 0.001	0.074 $\pm$ 0.001	0.075	0.073	<b>0.004</b> $\pm$ 0.001	<b>0.004</b> $\pm$ 0.002	<b>0.004</b> $\pm$ 0.001	0.008	<b>0.004</b>

## C.2 Additional Results on CIFAR-10-C

In this section, we provide additional experimental results on CIFAR-10-C. Table 3 is an extended version of Table 1, containing all severity levels 1-5. Figures 8, 9 and 10 show the loss, error and ECE, respectively, of the ensembles selected by NES and the baselines as a function of the budget  $K$ . For these ensembles, Figures 11 and 12 show the average base learner loss and the oracle ensemble loss, respectively. These plots generally show that NES algorithms find ensembles which outperform deep ensembles for almost all values of the budget  $K$ . Note that the error and ECE values in Table 3 correspond to the values at the rightmost end of the subplots in Figures 9 and 10, that is, when the budget  $K = 400$ .

We also include a variant of NES-RE, called NES-RE-0, in Figures 8, 9, 10, 11 and 12.<sup>4</sup> NES-RE and NES-RE-0 are the same, except that NES-RE-0 uses the validation set  $\mathcal{D}_{\text{val}}$  without any shift during iterations of evolution, as in line 4 of Algorithm 2. Following the discussion in Appendix B.3, recall that this is unlike NES-RE, where we sample the validation set to be either  $\mathcal{D}_{\text{val}}$  or  $\mathcal{D}_{\text{val}}^{\text{shift}}$  at each iteration of evolution. Therefore, NES-RE-0 evolves the population without taking into account dataset shift, with  $\mathcal{D}_{\text{val}}^{\text{shift}}$  only being used for the post-hoc ensemble selection step in line 9 of Algorithm 2.

As shown in the Figures 8 and 9, NES-RE-0 shows a minor improvement over NES-RE in terms of loss and error for ensemble size  $M = 30$  in the absence of dataset shift. This is in line with expectations, because evolution in NES-RE-0 focuses on finding base learners which form strong ensembles for in-distribution data. On the other hand, when there is dataset shift, the performance of NES-RE-0 ensembles degrades, yielding higher loss and error than both NES-RS and NES-RE. Nonetheless, NES-RE-0 still manages to outperform the DeepEnsembles baselines consistently. We draw two conclusions on the basis of these results: (1) NES-RE-0 can be a competitive option in the absence of dataset shift. (2) Sampling the validation set, as done in NES-RE, to be  $\mathcal{D}_{\text{val}}$  or  $\mathcal{D}_{\text{val}}^{\text{shift}}$  in line 4 of Algorithm 2 plays an important role in returning a final pool  $\mathcal{P}$  of base learners from which ForwardSelect can select ensembles robust to dataset shift.

Table 3: Extension of table 1. Error and ECE of ensembles on CIFAR-10-C for different shift severities and ensemble sizes  $M$ . Best values and all values within 95% confidence interval are bold faced.

Shift Severity	$M$	Classification Error (out of 1)					Expected Calibration Error (ECE)				
		NES-RS	NES-RE	DeepEns (RS)	DeepEns (DARTS)	DeepEns (AmoebaNet)	NES-RS	NES-RE	DeepEns (RS)	DeepEns (DARTS)	DeepEns (AmoebaNet)
0 (no shift)	5	<b>0.098</b> $\pm$ 0.001	<b>0.098</b> $\pm$ 0.002	0.112 $\pm$ 0.002	0.101	<b>0.098</b>	<b>0.012</b> $\pm$ 0.001	<b>0.013</b> $\pm$ 0.002	<b>0.011</b> $\pm$ 0.002	0.015	0.016
	10	<b>0.094</b> $\pm$ 0.001	<b>0.094</b> $\pm$ 0.002	0.108 $\pm$ 0.002	0.100	0.097	<b>0.012</b> $\pm$ 0.001	0.013 $\pm$ 0.001	<b>0.011</b> $\pm$ 0.001	<b>0.011</b>	0.013
	30	<b>0.092</b> $\pm$ 0.001	<b>0.092</b> $\pm$ 0.001	0.105 $\pm$ 0.002	0.095	0.094	0.012 $\pm$ 0.001	0.012 $\pm$ 0.001	0.012 $\pm$ 0.001	<b>0.011</b>	0.012
1	5	<b>0.163</b> $\pm$ 0.001	<b>0.164</b> $\pm$ 0.002	0.175 $\pm$ 0.004	0.172	0.172	<b>0.024</b> $\pm$ 0.001	0.027 $\pm$ 0.004	0.028 $\pm$ 0.001	0.038	0.040
	10	<b>0.158</b> $\pm$ 0.001	<b>0.159</b> $\pm$ 0.001	0.173 $\pm$ 0.004	0.169	0.166	<b>0.019</b> $\pm$ 0.001	<b>0.019</b> $\pm$ 0.003	0.023 $\pm$ 0.001	0.028	0.028
	30	<b>0.155</b> $\pm$ 0.001	0.157 $\pm$ 0.001	0.171 $\pm$ 0.004	0.164	0.163	<b>0.013</b> $\pm$ 0.001	0.015 $\pm$ 0.002	0.019 $\pm$ 0.002	0.020	0.021
2	5	0.196 $\pm$ 0.002	<b>0.192</b> $\pm$ 0.002	0.207 $\pm$ 0.005	0.214	0.212	<b>0.030</b> $\pm$ 0.002	<b>0.030</b> $\pm$ 0.004	0.039 $\pm$ 0.001	0.050	0.053
	10	<b>0.188</b> $\pm$ 0.001	<b>0.188</b> $\pm$ 0.002	0.203 $\pm$ 0.005	0.208	0.205	<b>0.019</b> $\pm$ 0.001	0.021 $\pm$ 0.003	0.031 $\pm$ 0.002	0.037	0.037
	30	0.186 $\pm$ 0.001	<b>0.184</b> $\pm$ 0.001	0.203 $\pm$ 0.005	0.206	0.201	<b>0.013</b> $\pm$ 0.001	0.015 $\pm$ 0.002	0.030 $\pm$ 0.002	0.031	0.029
3	5	0.238 $\pm$ 0.002	<b>0.233</b> $\pm$ 0.003	0.255 $\pm$ 0.007	0.266	0.267	<b>0.045</b> $\pm$ 0.002	<b>0.044</b> $\pm$ 0.002	0.062 $\pm$ 0.002	0.075	0.085
	10	0.232 $\pm$ 0.002	<b>0.229</b> $\pm$ 0.002	0.251 $\pm$ 0.007	0.263	0.256	<b>0.034</b> $\pm$ 0.001	<b>0.033</b> $\pm$ 0.002	0.052 $\pm$ 0.002	0.067	0.064
	30	0.231 $\pm$ 0.001	<b>0.228</b> $\pm$ 0.002	0.249 $\pm$ 0.007	0.258	0.252	<b>0.029</b> $\pm$ 0.001	<b>0.028</b> $\pm$ 0.002	0.049 $\pm$ 0.002	0.057	0.054
4	5	0.301 $\pm$ 0.002	<b>0.293</b> $\pm$ 0.004	0.316 $\pm$ 0.007	0.336	0.336	<b>0.079</b> $\pm$ 0.003	<b>0.077</b> $\pm$ 0.005	0.101 $\pm$ 0.001	0.125	0.133
	10	0.295 $\pm$ 0.001	<b>0.289</b> $\pm$ 0.003	0.313 $\pm$ 0.007	0.329	0.33	<b>0.068</b> $\pm$ 0.002	<b>0.067</b> $\pm$ 0.004	0.095 $\pm$ 0.002	0.109	0.116
	30	0.294 $\pm$ 0.001	<b>0.290</b> $\pm$ 0.003	0.311 $\pm$ 0.006	0.324	0.324	<b>0.064</b> $\pm$ 0.001	<b>0.063</b> $\pm$ 0.004	0.089 $\pm$ 0.003	0.100	0.103
5	5	0.387 $\pm$ 0.003	<b>0.376</b> $\pm$ 0.003	0.415 $\pm$ 0.011	0.429	0.438	<b>0.117</b> $\pm$ 0.004	<b>0.115</b> $\pm$ 0.008	0.152 $\pm$ 0.002	0.177	0.199
	10	0.380 $\pm$ 0.002	<b>0.374</b> $\pm$ 0.004	0.411 $\pm$ 0.009	0.429	0.427	<b>0.104</b> $\pm$ 0.004	<b>0.105</b> $\pm$ 0.007	0.144 $\pm$ 0.002	0.168	0.174
	30	0.382 $\pm$ 0.002	<b>0.375</b> $\pm$ 0.003	0.408 $\pm$ 0.009	0.427	0.422	<b>0.103</b> $\pm$ 0.002	<b>0.102</b> $\pm$ 0.006	0.136 $\pm$ 0.003	0.160	0.160

<sup>4</sup>The results shown are an average over 3 independent runs of NES-RE-0.

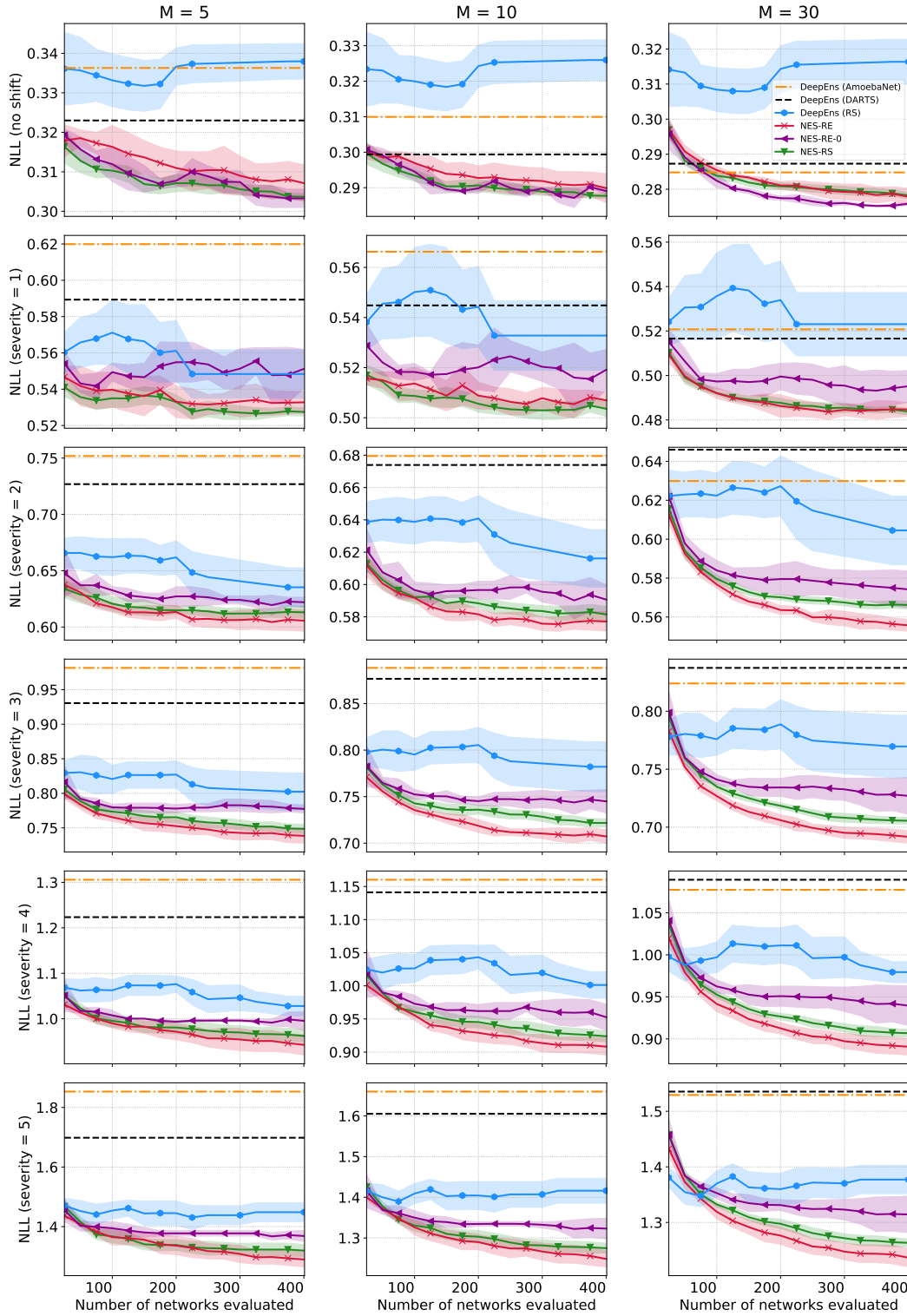


Figure 8: Results on CIFAR-10-C [24] with varying ensemble sizes  $M$  and shift severity. Lines show the mean NLL achieved by the ensembles with 95% confidence intervals. See Appendix C.2 for the definition of NES-RE-0.

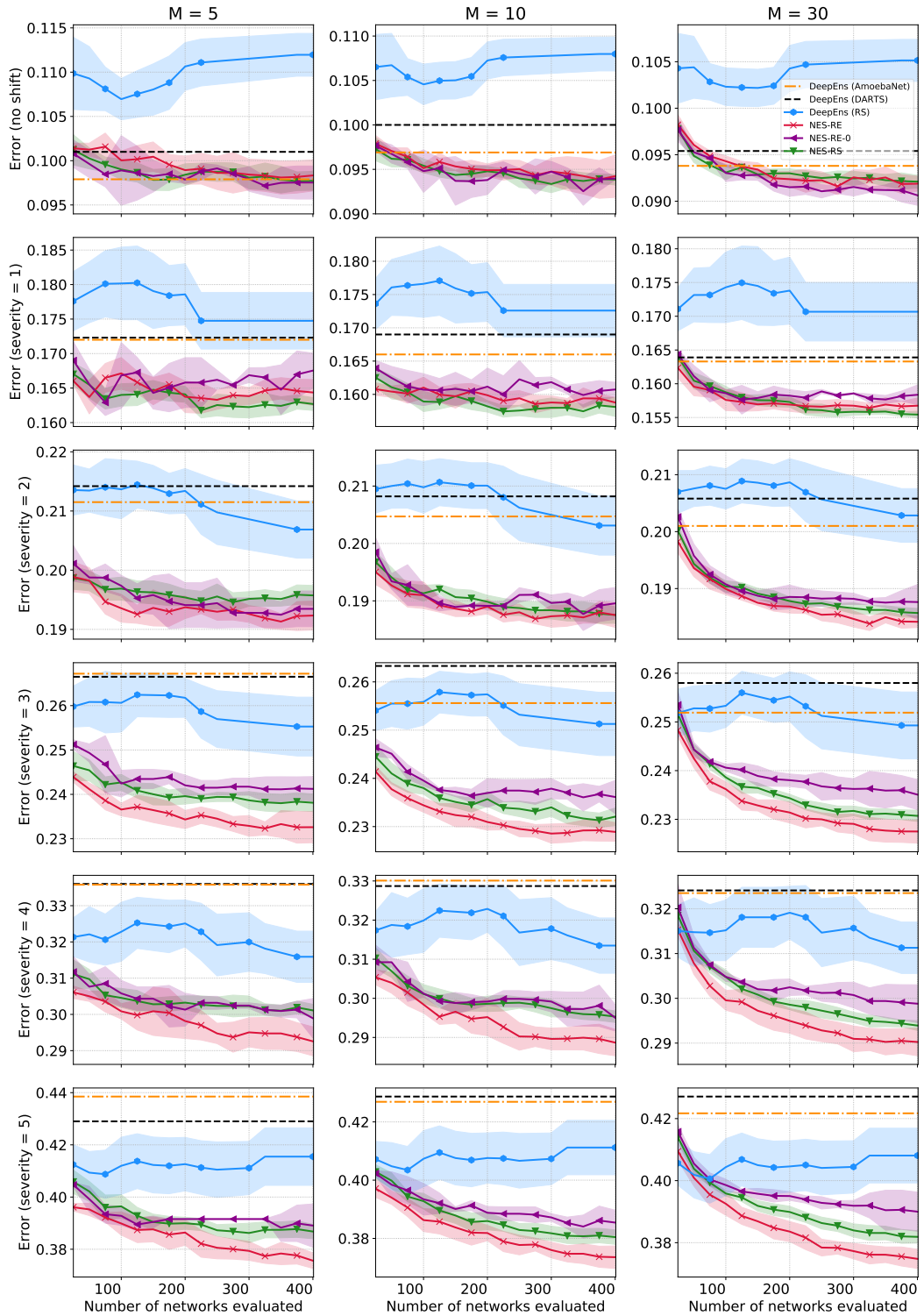


Figure 9: Results on CIFAR-10-C [24] with varying ensembles sizes  $M$  and shift severity. Lines show the mean error achieved by the ensembles with 95% confidence intervals. See Appendix C.2 for the definition of NES-RE-0.

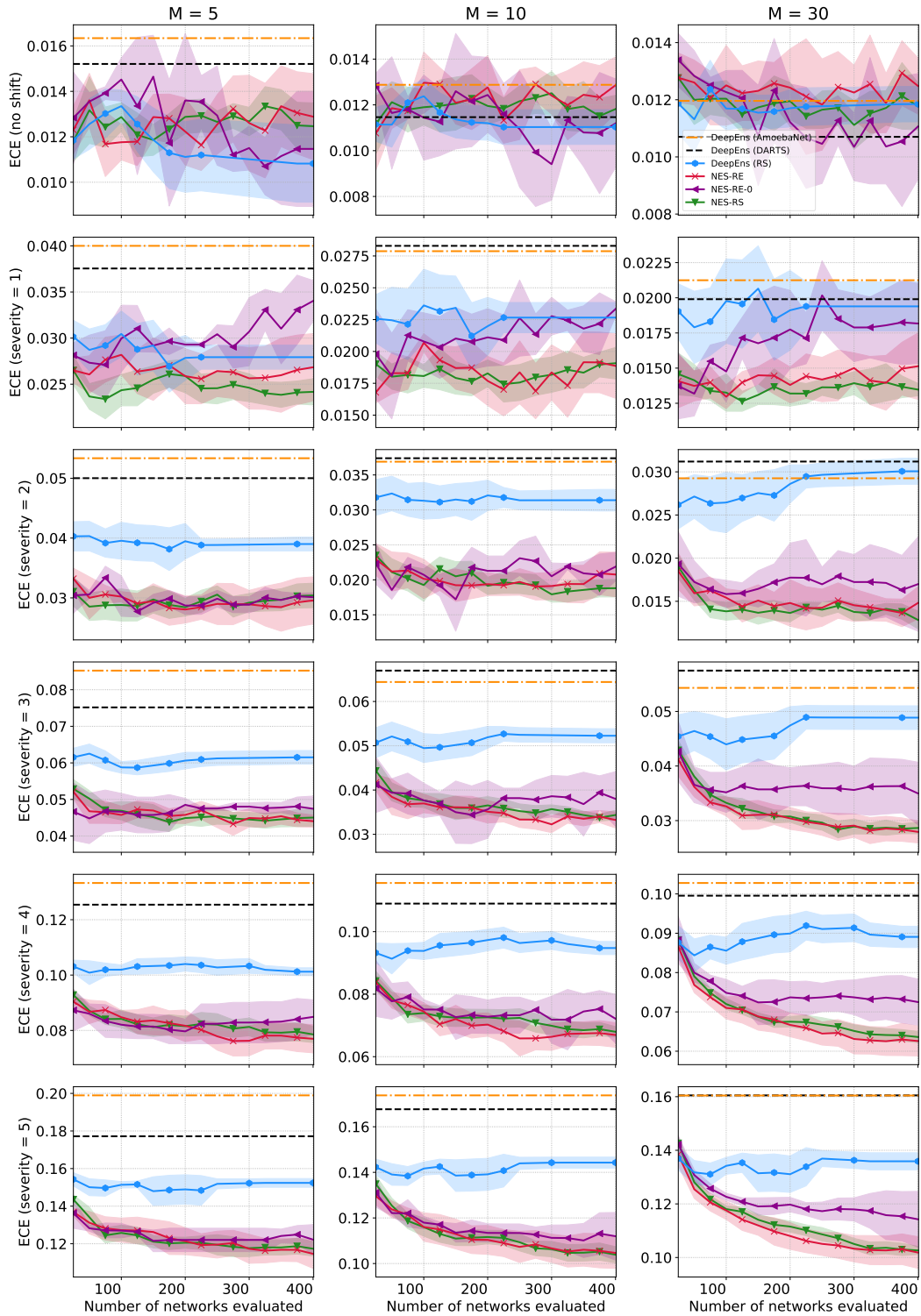


Figure 10: Results on CIFAR-10-C [24] with varying ensemble sizes  $M$  and shift severity. Lines show the mean ECE achieved by the ensembles with 95% confidence intervals. See Appendix C.2 for the definition of NES-RE-0.

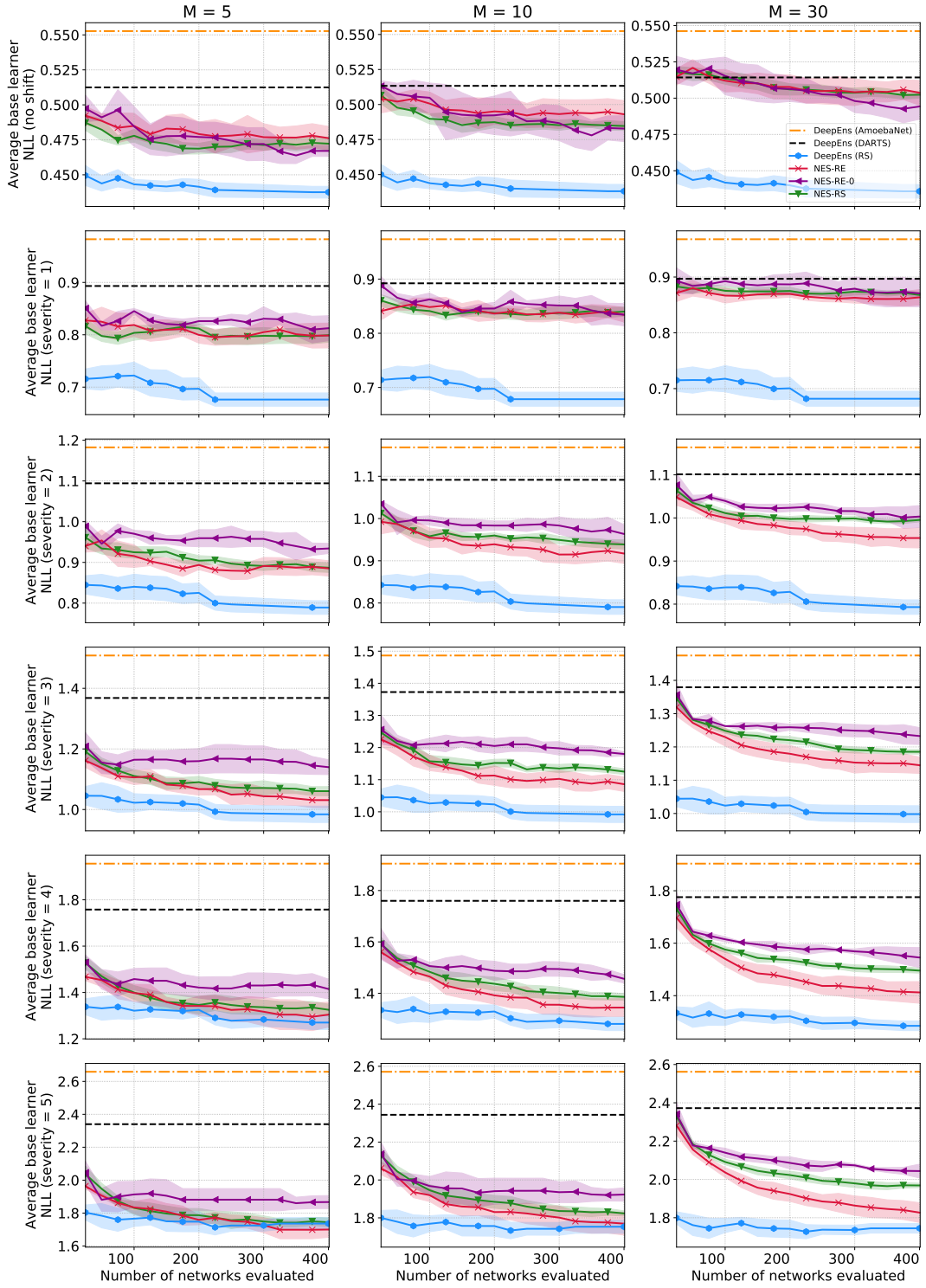


Figure 11: Results on CIFAR-10-C [24] with varying ensemble sizes  $M$  and shift severity. Lines show the mean of the average base learner loss with 95% confidence intervals. See Appendix C.2 for the definition of NES-RE-0.

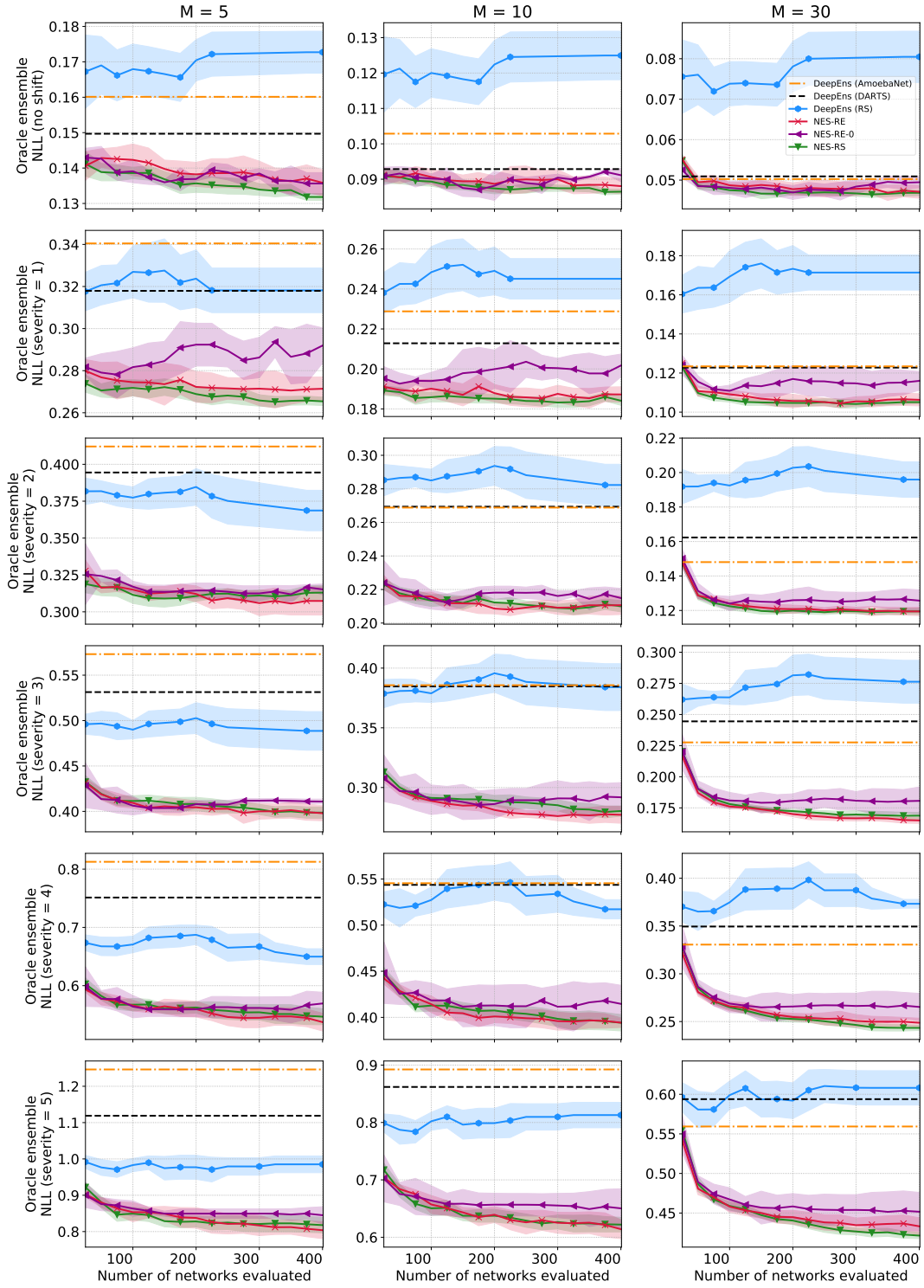


Figure 12: Results on CIFAR-10-C [24] with varying ensembles sizes  $M$  and shift severity. Lines show the mean of the oracle ensemble loss with 95% confidence intervals. See Appendix C.2 for the definition of NES-RE-0.